Int. J. Electrochem. Sci., 14 **(2019)** 7570 – 7581, doi: 10.20964/2019.08.20

International Journal of
ELECTROCHEMICAL
SCIENCE
www.electrochemsci.org

Short Communication

Effect of Microstructure on Wear Resistance of Low-Alloy High-Strength Wear-Resistant Steel

Dongting Wu[1], *Hui Zhang*[1, 2], *Shushuai Liu*[1], *Yuanxiao Li*[3], *Zhiqiang Li*[4,*] *Yong Zou*[1*]

[1] Key Laboratory for Liquid-Solid Structural Evolution and Processing of Materials, Ministry of Education, Shandong University, Jinan 250061, China
[2] School of Mechanical and Automotive Engineering, Qilu University of Technology, Jinan 250353, China
[3] Shandong Institute for Products Quality Inspection, Jinan 250100, China
[4] Center for Optics Research and Engineering (CORE), Shandong University, Qingdao 266237, China.
[*]E-mail: yzou@sdu.edu.cn

Received: 8 March 2019 / *Accepted:* 29 May 2019 / *Published:* 30 June 2019

In this paper, microstructure, corrosion resistance and wear resistance of low-alloy high-strength wear-resistant steels of NM400 and KN400X were studied. It is found that the wear resistance of these steels differed from each other significantly although their chemical compositions were similar, depending on microstructure, grain size and non-metallic inclusions. The results of the tests on corrosion resistance and wear resistance showed that the KN400X steel had the best performance in both properties. Lower content of non-metallic inclusions resulted in more uniform and compact microstructure, which together with better corrosion resistance led to better abrasive wear property.

Keywords: wear resistance; microstructure; Electrochemical; corrosion resistance

1. INTRODUCTION

Due to the excellent mechanical properties, low alloy high strength wear-resistant steels are extensively applied for civilian purposes, such as vehicles, ships, metallurgy, and engineering machinery[1, 2]. In order to improve the hardenability of low alloy high strength wear-resistant steels, micro-alloying elements are widely used [3, 4]. Meantime, Quenching and low temperature tempering are applied to improve strength and wear resistance [5-7]. The most widely used wear-resistance steels are steels with Brinell hardness of approximately 400, such as HARDOX400 produced in Sweden, NM400 produced in China, and FK400 produced in Japan[8]. Although they are similar in chemical compositions, their hardness and wear resistance differ from each other due to different manufacturing processes [7, 9]. On the other hand, the reports about electrochemical corrosion of wear-resistant steels

were seldom.

In this paper, NM400 and KN400X wear-resistant steels were compared. The chemical composition, microstructure, non-metallic inclusions (cleanliness), corrosion resistance and wear resistance were measured. This study focused on identifying the difference in wearing resistance between the steels of the two types and the effects of influence factors on the difference.

2. EXPERIMENTAL METHODS

In this paper, four types wear-resistant steel were contrastive studied. One was a KN400X steel produced by Japan, marked as R. The other three were all NM400 steels from different companies of China, marked as B, S and J.

The chemical compositions were examined by using a BAIRD One Spark direct-reading spectrometer, and argon with purity more than 99.99% was used as the working gas. The testing positions were 1/4 thickness below the surface.

The surface microstructure was observed on the latitudinal section of the steels by using a KEYENCE VHX-500FE digital microscope. The wear morphology was observed by using a CARL ZEISS EVO MA 10 scanning electron microscopy (SEM), with the accelerating voltage of 20.0 kV.

The content of non-metallic inclusions was measured according to the testing method for the non-metallic inclusions in steel specified in JIS G0555-2003 Microscope. The results were obtained by using an Olympus GX51 inverted metallurgic microscope using point counting method. The number of visual fields was 60 and the magnification was 400.

The surface hardness was measured by using a HVS-50 Vickers hardness tester under a 294.2N load.

The corrosion tests were performed in the potentiodynamic polarization and electrochemical impedance spectroscopy (EIS). The measurements were made using a CS350 electrochemical workstation, connected to a three-electrode electrochemical cell. The polarization curves were measured using 3.5 wt% NaCl solution at room temperature. A saturated calomel electrode (SCE) was used as the reference electrode, and a platinum electrode was used as the counter electrode. The samples of the steels were used as the working electrodes. Before tests, the samples were immersed in the electrolyte for about 20min to stabilize the open-circuit potential (OCP). The potentiodynamic polarization tests were conducted with a scan rate of 1 mV/s. The initial potential was -0.5V, and the termination potential was +1.5V. The excitation signal of electrochemical impedance spectroscopy was a sinusoidal wave with an amplitude of 10 mV. The frequency span was from 100 kHz down to 0.01 Hz. EIS curve was fitted by Zsimwin software.

The wear resistance was evaluated by using a MLS-225 wet sand rubber wheel abrasive wear tester. The dimensions of specimens for abrasive wear test were 30mm×7mm×7 mm, and the surface of specimens was polished by abrasive papers. The abrasive material was silica sand with a diameter of 220–450 μm. The slurry was composed of 1.0 kg of water and 1.5 kg of silica sand. The load on wear specimens was 100 N. The rubber wheel revolved at a speed of 240 r/min. Preliminary grinding was carried out for 1000 revolutions with accurate grinding for 2000 revolutions 3 times. The weight of the

specimens before and after accurate grinding was recorded using a JJ224BC analytical balance to an accuracy of 0.1 mg. The difference was weight loss due to abrasive wear.

3. RESULTS

3.1. Chemical Composition

Table 1. The chemical composition (wt. %) of the steels

Steel	C	Si	Mn	S	P	Cr	Mo	Cu	Al	W
R	0.143	0.224	1.369	0.002	0.014	0.005	0.019	0.012	0.032	0.034
J	0.139	0.209	1.374	0.003	0.013	0.165	0.173	0.020	0.033	0.041
S	0.176	0.282	1.410	0.002	0.013	0.164	0.160	0.020	0.033	0.040
B	0.183	0.346	1.400	0.008	0.016	0.013	0.019	0.015	0.019	0.017

The chemical composition of the steels used is presented in **Table 1**. As is shown, the five important alloy elements especially the Si, Mn, S and P elements exhibited a homogenous content, and only C element varied slightly. The carbon content in steel J was the lowest and that of Steel B was the highest, showing a dissimilarity of 0.04%. C element plays an important role in improving the hardness and wear resistance [10, 11]. However, the carbon content gap of no more than 0.04% may be ignored for high strength wear-resistant steels with carbon content not exceeding 0.20%. Compared to steels R and B, steels J and S had more contents of Cr and Mo elements, with the largest Cr content up to 33 times and the largest Mo content 9 times those of the other two. Cr element contributes to carbide formation and improvement of the hardenability[12]. Mo element is more efficient in increasing the hardenability. Besides, Mo element can reduce the temper brittleness caused by other elements [13, 14]. Therefore, it can be deduced that steel J and S are propitious to generate martensite.

3.2. Microstructure

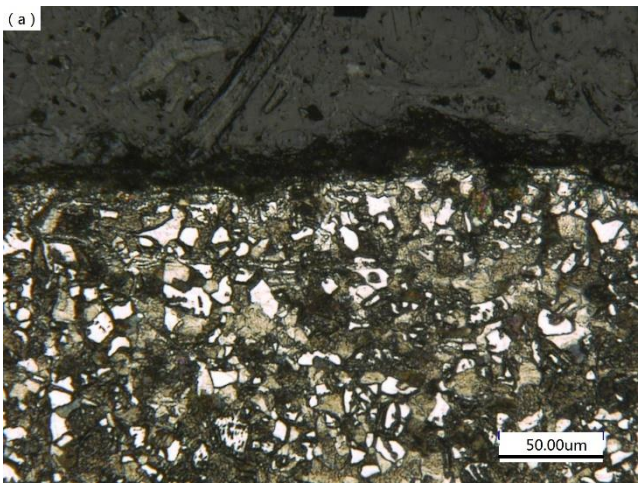

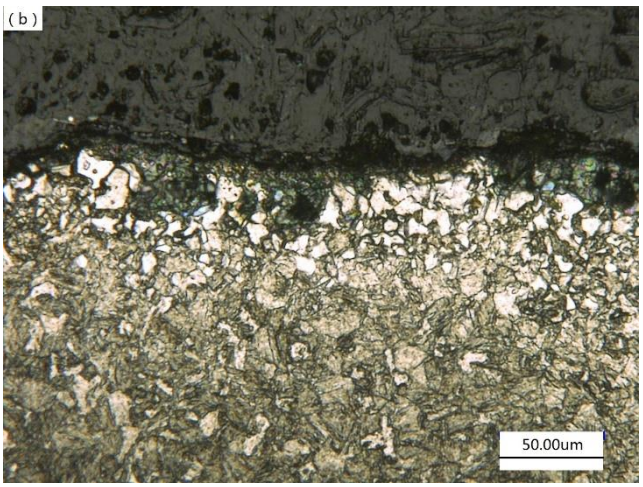

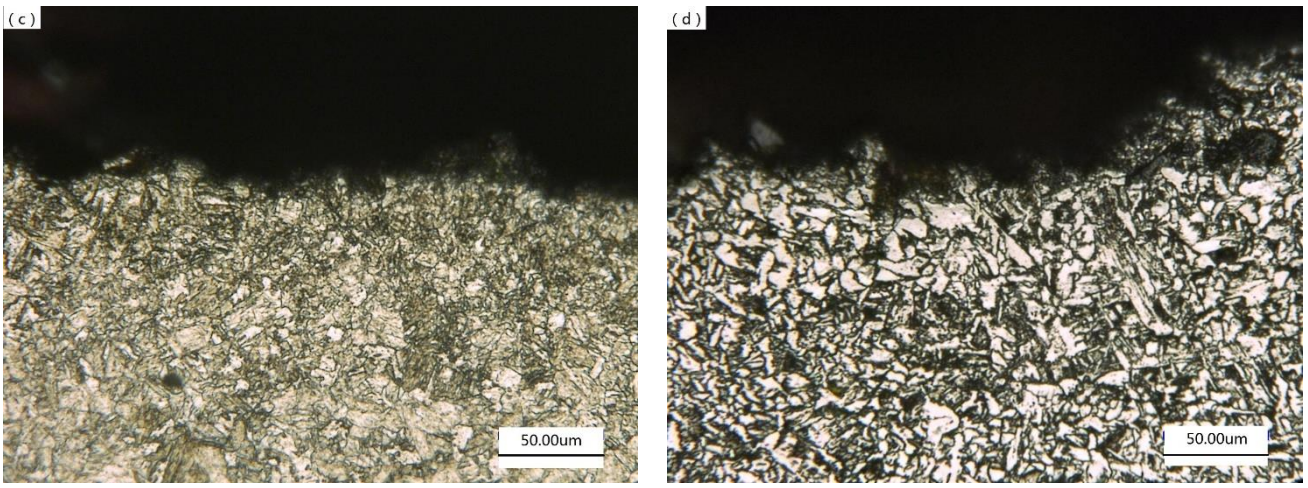

Figure 1. The surface microstructure of steels (a) R (b) J (c) S (d) B

Figure 1 shows the surface metallograph of these steels. According to the photos, the surface of steel R is tight and smooth. The microstructure is tempered martensite [Figure 1.R]. The microstructure of steel J is tempered martensite, bainite and residual austenite [Figure 1.J]. Furthermore, there is decarburization in the surface of steel J. The surface roughness of steel S is much higher, and the microstructure is tempered martensite and bainite [Figure 1.S]. The microstructure of steel B is martensite, bainite and residual austenite [Figure 1.B] with the highest surface roughness.

3.3. The Content Of Non-Metallic Inclusions

The non-metallic inclusions may deteriorate the mechanical properties of steel, especially the plasticity, toughness and endurance limit. Inclusions of different shapes scatter in the metal, which destroy the continuity and integrity of the metal. The non-metallic inclusions in Group A (sulfide type) and Group C (silicate type) present a wide range of aspect ratios (length/width), seriously split the matrix, and lead to reduction of bearing capacity. The non-metallic inclusions in Group B (aluminate type) and Group C are fragile, and they may break up when the matrix distorts. The non-metallic inclusions in Group C may give rise to fatigue cracks because of their sharp ends. At the same time, the non-metallic inclusions can result in surface degradation and decreased life of components[15].

Table 2. The content of non-metallic inclusions in the steels

Steel	d(A)60×400	d(B+C)60×400	d(total)60×400
R	0.002	0.003	0.005
J	0.006	0.014	0.020
S	0.007	0.012	0.019
B	0.011	0.025	0.036

The contents of non-metallic inclusions in different steels are shown in Table 2. Steel R is cleanest with minimum non-metallic inclusions of the three types. Steel B contains the maximum non-

metallic inclusions with the content seven times that in steel R according to the total amount. In this aspect, steels J and S seem better than steel B. Nevertheless, the content is four times that of steel R. Compared to steel R, steel B, J and S are easy to be peel off in the superficial zone during friction, which will aggravate abrasive wear.

3.4. Surface Hardness

The surface hardness plays a significant role in the wear resistance. For the cutting wear, higher surface hardness can distinctly improve the wear resistance. However, higher surface hardness may be not necessarily good for impact wear[16]. Higher surface hardness may decrease the toughness of steel. Figure 2 shows the surface hardness results.

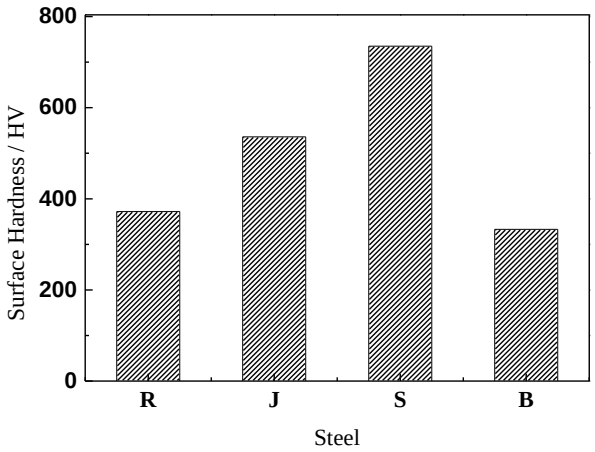

Figure 2. The surface hardness of the four steels

As shown in this figure, the surface hardness of steel R and B is less than half of the hardness of steel S. If only the surface hardness is considered, the surface of steel R and B may crush, and groove or furrow may be formed accordingly in abrasive wear environment without impact. But in the wear environment with vibration, the surface of steel S may be brittle and peel off due to the higher surface hardness.

3.5. Wearability Test

Figure 3 shows the results of the wear resistance. It can be seen that the weight loss of all steels accelerates with the extension of time. From the results of vertical comparison, it can be found that the weight loss of steel R is minimal in every period. After 700-revolution wear test, the weight loss is only a little more than that of steel J receiving a 3000-revolution test, and even less than half of that of steel S receiving a 3000-revolution test.

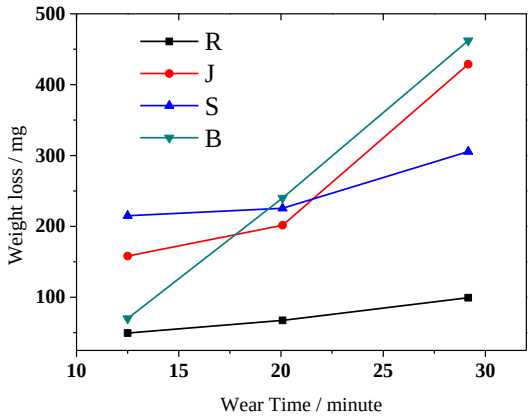

Figure 3. The wet sand rubber wheel abrasive wear loss of the steels

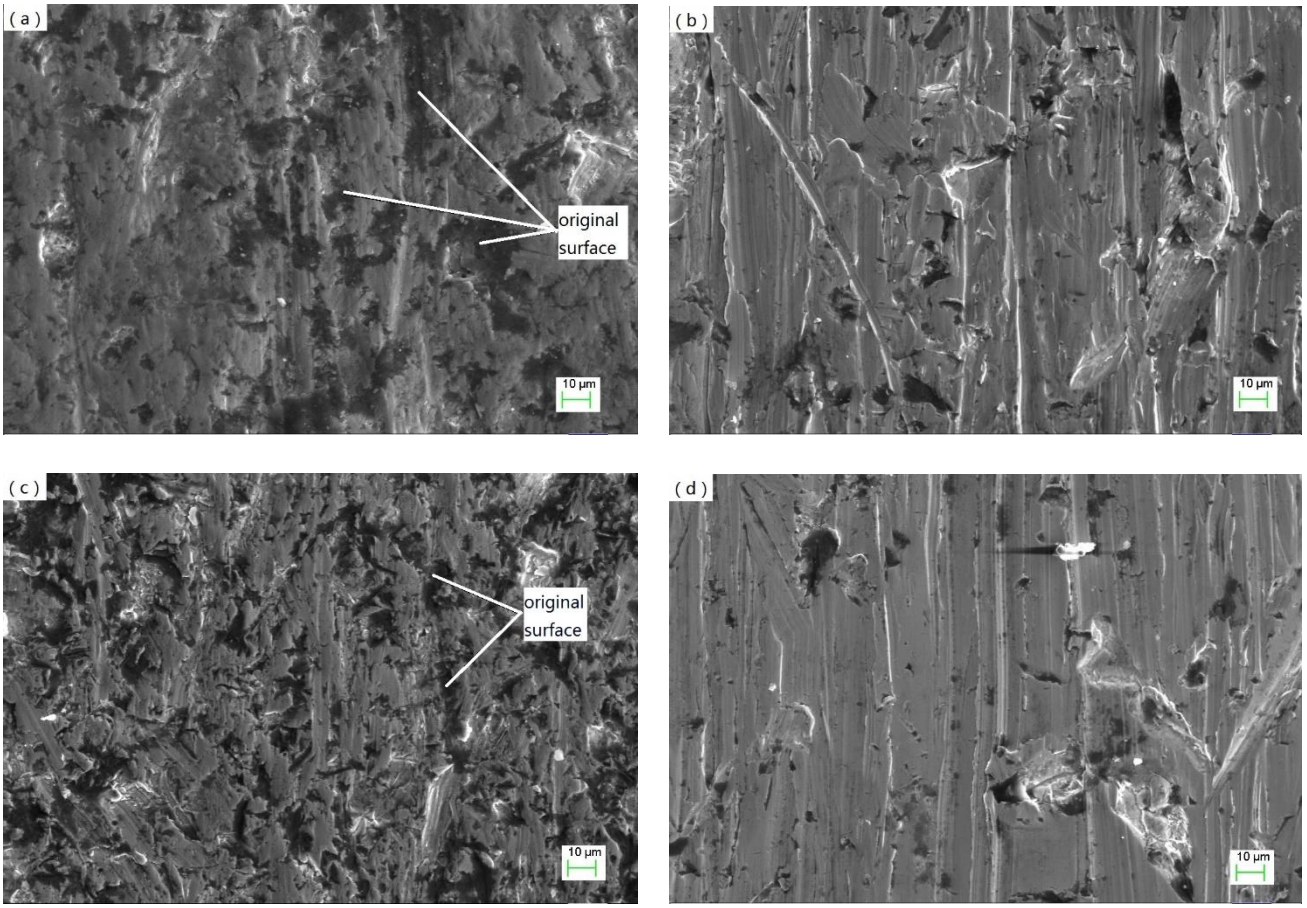

Figure 4. The morphology after wet sand rubber wheel abrasive wear test of the steels (a) R (b) J (c) S (d) B

For the steels of NM400, the weight loss of steel B is the lowest after the initial 3000-revolution test, but the weight loss is the most serious after 500-revolution test. The weight loss of steel S is the

highest after the primary 3000-revolution tests, but the loss reduced in the subsequent tests. After 7000-revolution tests, the weight loss is much lower than the other two.

The morphologies after abrasive wear tests are shown in Figure 4. As shown in this figure, there are slight cutting grooves on the surface of steel R, with keeping a large quantity of original surface without obvious wear traces. Discontinuous cutting grooves appeared on the surface of steel S where only a little initiative surface can be found. The surface of steel J and B was seriously damaged with deep and wide continuous furrows.

3.6. Corrosion Experiments

Figure 5 shows the open-circuit potential curves of the steels in 3.5 wt% NaCl solution. It can be seen that the open-circuit potential of four steels are different. The open-circuit potential of J sample is the highest, and the change range of R sample is the smallest within 20 minutes of testing.

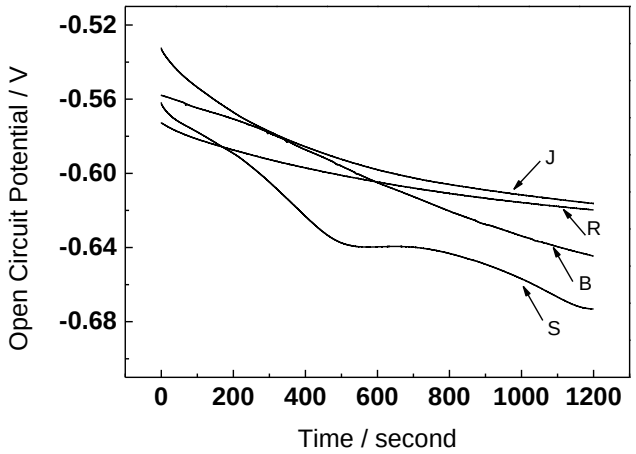

Figure 5. The open-circuit potential curve of the steels in 3.5 wt% NaCl solution

Figure 6 shows the potentiodynamic polarization curves of the steels in 3.5 wt% NaCl solution. The parameters of potentiodynamic polarization are fitted by traditional Tafel method as shown in Table 3.

Table 3. Fitting results of the polarization curves in 3.5 wt% NaCl solution

Steel	I_{corr} ($\mu A/cm^2$)	E_{corr} (V)	Corrosion rate (mm/yr)
R	10.237	-0.782	0.120
J	13.435	-0.722	0.158
S	115.791	-0.872	1.362
B	117.912	-0.807	1.387

From Fig.6, it can be seen that there is obvious passive phenomenon in anion polarization of all these steels. The widest passive area is S sample while the narrowest passive area is R sample. All the

steels are reactivated at the voltage from -0.6V to -0.5V. From the fitting results in Table 3, it is known that the corrosion potential (E_{corr}) of steels R and J is a little higher than the other two steels, but the corrosion current density (I_{corr}) and the corrosion rate are much lower than the other two. The I_{corr} and corrosion rate of steel B are more than 11.5 times that of steel R.

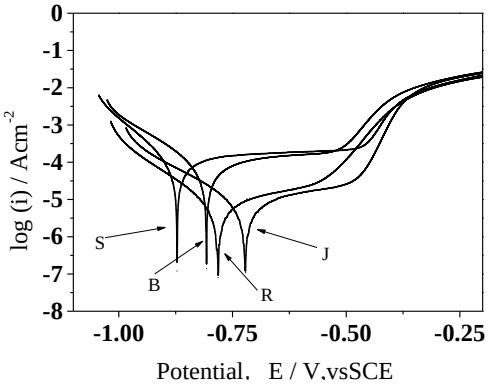

Figure 6. The polarization curve of the steels in 3.5 wt% NaCl solution

Figure 7 shows the electrochemical impedance Nyquist diagram of the steels in 3.5 wt% NaCl solution. The EIS Nyquist curves of the four steels are similar in shape and all of them show capacitive arc resistance in the first quadrant. The capacitive arc radius of S and J samples is obviously larger than that of R and B, which means that S sample has the better corrosion resistance. Figure 8 shows high frequency band of the four EIS Nyquist curves in 3.5 wt% NaCl solution. It can be found that the Nyquist curves of four samples have a section of capacitive arc resistance at high frequencies, and the radius of the curves is obviously different from that at low frequencies. This shows that the Nyquist patterns of four steels have two time constants. R_S (Q_fR_f) ($Q_{Ct}R_{Ct}$) as shown in Figure 9 is selected as the equivalent circuit to fit the Nyquist Atlas of the four samples. The parameters of each element in the equivalent circuit are summarized in Table 4. From the fitting results, we found that the shape of EIS Nyquist spectra of the four samples is similar, but the parameters of the equivalent circuit elements are obviously different. The resistance Rf of corrosion product film of R and B samples is only 1/150 of that of steel S and J.

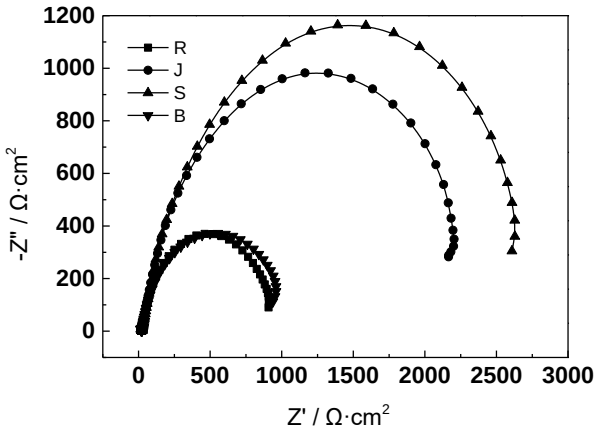

Figure 7. Electrochemical impedance Nyquist diagram of the steels in 3.5 wt% NaCl solution

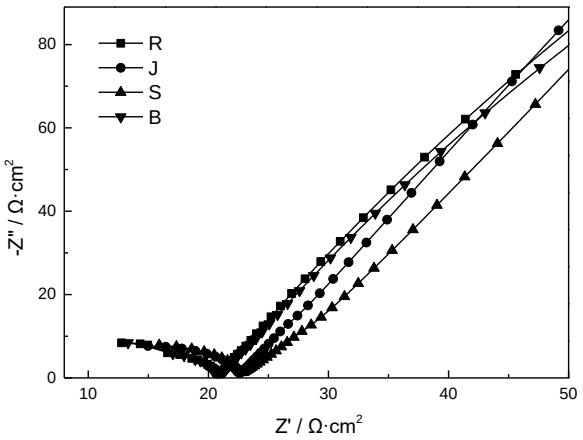

Figure 8. Electrochemical impedance Nyquist diagram of the steels of high frequency band

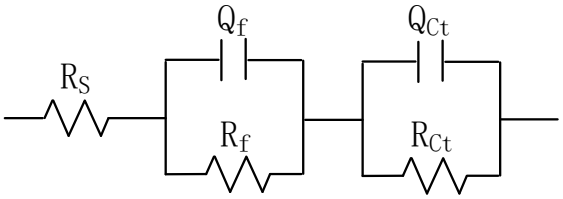

Figure 9. Equivalent circuit of the steels in 3.5 wt.% NaCl solution

Table 4. Fitting results for EIS of the steels in 3.5 wt.% NaCl solution

Steel	R_S(Ω cm^2)	R_f(Ω cm^2)	Q_f		R_{Ct}(Ω cm^2)	Q_{Ct}	
			Y_f(μ Fcm^{-2})	n_1		Y_{Ct}(μ Fcm^{-2})	n_2
R	4.78	15.95	8.25E-8	1	942	7.45E-4	0.84
J	5.73	2415	3.42E-3	0.84	17.11	1.99E-7	0.93
S	4.07	2982	4.66E-3	0.82	23.72	5.43E-7	0.80
B	5.06	15.72	9.14E-8	1	1008	7.93E-4	0.82

4. DISCUSSION

By comprehensively comparing the chemical composition, microstructure, non-metallic inclusions, surface hardness, corrosion and wear resistance, it can be found that the chemical composition of the four types of steels seems similar, but the corrosion resistance and wear resistance were obviously different. Although the surface of steel R is not the hardest, its abrasive wear resistance is much better than the other samples.

The wear mechanisms are various, but they can be divided into the following three types: (1) cutting wear. When exposed to wear environment with hard abrasive, the surface of steel may be stabbed by the abrasive with vertical force, and the grooves leave behind owing to slide with horizontal force. The weight loss of cutting wear depends on the surface hardness. Harder surface contributes to lower weight loss caused by cutting wear. (2) fatigue wear. The fatigue wear can be divided into deformation

fatigue wear and delamination fatigue wear. Deformation fatigue wear is usually accompanied by low cycle fatigue. The wear resistance depends on the hardness and plasticity or toughness. Delamination fatigue wear occurs in the deformation and hardening of the matrix under the action of soft or hard abrasive. Due to the effect of contact stress, the cracks generate in the sub surface layer. If the cracks extend to the surface, the thin hardened layers will peel off. This type of wear is related to stress fatigue. The wear resistance depends on the hardness and toughness. (3) Brittle fracture wear. In the conditions of hard abrasive and impact, brittle fracture and delamination may take place in the brittle phase (such as carbide) or brittle matrix (such as martensite). This type of wear is directly related to the impact toughness and fracture toughness of the material. In general, all types of wear mechanisms occur simultaneously, and they are merely in different ratio as the operating conditions are diverse. By analyzing wear mechanisms, it can be found that the surface hardness is not the only influence factor, and the uniformity of the microstructure also plays an important role in the wear resistance[17].

The above electrochemical test results show that the corrosion resistance of these steels is also different. Ilyas Hacisalihoglu[18]reported the corrosion potential of Hardox 400 is about -0.60V in 3.5% NaCl solution and there is no obvious passivation in polarization curve, which is similar to the result of steel R in this study. It is well known that the corrosion potential mainly depends on the composition, and the corrosion current is related to the microstructure[19]. Although there was more Cr in steel S, the corrosion potential was the lowest. It is possible that Cr didn't dissolve in the substrate of S sample but form carbides to improve the hardness. Meanwhile, it can be found that steel S is the hardest one in the test of surface hardness. From the polarization curve, S and J samples have a wide passivation range, which is attributed to the high content of Cr and Mo elements in S and J, which leads to the formation of a stable passivation film on the surface of steel during electrochemical reaction and slows down the corrosion process[20] .

The difference in the corrosion current density reflects the uniformity of the steel. The larger corrosion current density implies that there are more micro cells caused by the potential difference between the heterogeneous phase and the substrate[21]. The corrosion current density of steel R is the smallest means that the microstructure of this steel is the most uniform.

The electrochemical impedance Nyquist spectra of four kinds steel show two time constant capacitive arc resistance. This is mainly caused by the difference between the surface and inner structures during rolling process for producing these low alloy high strength wear resistant steels. The surface structure formed by rapid cooling and other reasons is different with the inner structure. And the surface thickness is very thin, so it only shows a less obvious capacitive arc resistance.

The resistance R_f of corrosion product film of R and B samples is much lower than that of S and J, while the charge transfer resistance R_{Ct} of R and B is significantly higher than that of the other two. This is mainly because the measurement of EIS satisfies the "stability condition". The disturbance is small and the reaction on the electrode surface is not too enough. S and J samples with more Cr and Mo elements have enough time to form a stable passivation film on the surface and improve the resistance R_f of the corrosion product film. However, in the actual wet sand rubber wheel abrasive wear test, there will not be enough time to achieve "stability conditions" and form a stable passive film, so the corrosion resistance of S and J samples during the wear test process is not good.

As can be seen from the above analysis of wear mechanisms, higher surface hardness will improve the wear resistance of cutting wear, but it maybe not good for fatigue wear and brittle fracture wear[11]. The surface of steel B is soft, so its cutting wear resistance is poor. Moreover, the corrosion current density of steel B is so high and there are large quantities of non-metallic inclusions in steel B, and the spalling of the non-metallic inclusions may aggravate the wear of the matrix. Therefore, the wear of steel was the most serious with obvious distortion furrows and cutting grooves.

The surface of steel S is the hardest with the best resistance of abrasive stabbing and cutting. There were few distortion furrows and cutting grooves on the surface. However, excessively hard surface will easily be involved in brittleness fracture and micro-spalling, which leading to the highest weight loss at the initial wear stage. As shown by the wear morphology, a great deal of wear potholes may be caused by the delamination in the brittle phase.

J sample has excellent corrosion resistance and moderate surface hardness, but the weight loss is still high. Poor wear resistance might be attributable to the unsatisfactory cleanliness and the decarburization on the surface. The local area with decarburization would cause the occurrence of soft spots, which would be easily stabbed by abrasive and result in cutting and distortion wear.

R sample has much better wear resistance than that of the other samples, which was due to the synthetic action of cleanliness, microstructure and corrosion. Better cleanliness contributes to more excellent combination properties. The moderate surface hardness and the fine tempered martensite prevent the abrasive stabbing which may result in the rejection of cutting and delamination. Fine grain and maximum cleanliness will abate the fatigue wear, and better corrosion resistance will prevent wear caused by pitting.

5. CONCLUSIONS

For the low alloy high strength wear-resistant steel, the wear resistance is not entirely consistent with the surface hardness. The wear resistance is determined by a combination of chemical composition, microstructure and the non-metallic inclusions.

The non-metallic inclusions play a significant role in the wear resistance, and the delamination of inclusions will aggravate the wear. Higher surface hardness is not always conducive to wear resistance if the spalling of brittle phase caused by brittle fracture wear cannot be avoided. Therefore, it should be considered the species and distribution of strengthening phase more than the surface hardness.

The electrochemical results shown that the corrosion resistance not only depends on the compositions, but also affects by the microstructure. The better corrosion resistance can improve the wear resistance of steel by reducing the opportunity of pitting.

ACKNOWLEDGEMENTS
This project is supported by National Natural Science Foundation of China (No. 51271099).

References

1. I.M. Hutchings, *Materials Science and Engineering:* A, 184 (1994) 185-195.
2. D. Tanigawa, N. Abe, M. Tsukamoto, Y. Hayashi, H. Yamazaki, Y. Tatsumi, M. Yoneyama, *Optics And Lasers In Engineering,* 101 (2018) 23-27.
3. I. Mejía, A. Bedolla-Jacuinde, J.R. Pablo, *Wear,* 301 (2013) 590-597.
4. J. Chen, B. Ma, S. Feng, Y. Dai, G. Liu, H. Song, L. Jia, *Surface Engineering*, 35 (2019) 351-359.
5. C. Chattopadhyay, S. Sangal, K. Mondal, A. Garg, *Wear,* 289 (2012) 168-179.
6. B.K. Prasad, S.V. Prasad, Wear, 151 (1991) 1-12.
7. Y. Cao, Z.-d. Wang, J. Kang, D. Wu, G.-d. Wang, *Journal of Iron and Steel Research, International,* 20 (2013) 70-75.
8. H.-y. Song, C.-m. Li, L.-y. Lan, D.-w. Zhao, G.-d. Wang, *Journal of Iron and Steel Research, International,* 20 (2013) 72-77.
9. Z.-q. Jiang, J.-m. Du, X.-l. Feng, *Journal of Iron and Steel Research, International,* 13 (2006) 57-61.
10. J.C. Rawers, *Wear*, 258 (2005) 32-39.
11. H. Zhang, D. Wu, T. Luan, G. Xiao, W. Zhao, *International Journal Of Electrochemical Science,* 14 (2019) 2208-2215.
12. S. Hanke, A. Fischer, J.F. dos Santos, *Wear*, 338–339 (2015) 332-338.
13. M.I. De Barros, J. Bouchet, I. Raoult, T. Le Mogne, J.M. Martin, M. Kasrai, Y. Yamada, *Wear*, 254 (2003) 863-870.
14. J. Burbank, M. Woydt, *Wear*, 338–339 (2015) 133-143.
15. H. Krause, C. Schroelkamp, *Wear*, 120 (1987) 353-367.
16. I. Konyashin, B. Ries, D. Hlawatschek, Y. Zhuk, A. Mazilkin, B. Straumal, F. Dorn, D. Park, *International Journal of Refractory Metals and Hard Materials,* 49 (2015) 203-211.
17. Y. Liu, J.M.C. Mol, G.C.A.M. Janssen, *Scripta Materialia*, 107 (2015) 92-95.
18. I. Hacisalihoglu, F. Yildiz, A. Celik, *Tribology International*, 120 (2018) 434-445.
19. H. Zhang, K. Chong, G. Xiao, Z. Sun, W. Zhao, *Surface & Coatings Technology*, 352 (2018) 222-230.
20. Y. Qiu, S. Thomas, D. Fabijanic, A.J. Barlow, H.L. Fraser, N. Birbilis, *Materials & Design*, 170 (2019).
21. A. Evangeline, P. Sathiya, *Materials Research Express,* 6 (2019).